Hindawi Publishing Corporation
Journal of Nanotechnology
Volume 2016, Article ID 1746908, 5 pages
http://dx.doi.org/10.1155/2016/1746908

Research Article

The Repulsive Casimir Force with Metallic Ellipsoid Structure

Yujuan Hu,[1,2] Ruo Sun,[3] Zhixiang Huang,[1] and Xianliang Wu[1]

[1]*Key Laboratory of Intelligent Computing & Signal Processing, Anhui University, Ministry of Education, Hefei 230039, China*
[2]*Department of Education, Hefei Normal University, Hefei 230601, China*
[3]*Anhui Measuring Science Research Institute, Hefei 230051, China*

Correspondence should be addressed to Zhixiang Huang; zxhuang@ahu.edu.cn

Received 5 May 2016; Revised 25 July 2016; Accepted 18 August 2016

Academic Editor: Oded Millo

We propose a new structure, one plate with a hole above the ellipsoid and the other plate with a hole below the ellipsoid, to obtain a repulsive Casimir force. The force was obtained numerically by using the in-house FDTD method, based on Maxwell's stress tensor and harmonic expansion. The code can be verified by calculating the force of a perfect-metal ellipsoid centered above a perfect-metal plate with a hole. Our numerical method can effectively simulate the Casimir force by reducing the total simulated time. The further numerical results of realistic dielectric material immersing in fluids or adding other plates above the ellipsoid are also presented. It is not surprising to find that the larger differences can be achieved by varying the parameters such as the center-center separation, medium immersed, and the dielectric material of the structure. Thus, it is possible to tune these parameters relatively in the realistic microelectromechanical systems to overcome stiction and friction problems.

1. Introduction

The Casimir force [1], arising from quantum fluctuations of the electromagnetic field, has been widely studied over the past decades [2, 3]. Nowadays Casimir force plays a pivotal role in "stiction," which is indispensable to the progress in the field of nanotechnology [4], especially in the fabrication of microelectromechanical systems (MEMS).

An idealized geometry was established in vacuum [5], a perfect-metal ellipsoid centered above a perfect-metal plate with a hole, as depicted in Figure 1. The repulsive phenomenon occurs when the plate is close to the ellipsoid. The ellipsoid was assumed to be electrically polarizable only in the z direction. When the plate lies in the $z = 0$ plane, the Casimir-Polder energy for such an ellipsoid at position x is

$$U(x) = -\frac{1}{2\pi}\int_0^\infty \alpha_{zz}(i\xi)\left\langle E_z(x)\,E_z(x)\right\rangle_{i\xi} d\xi, \qquad (1)$$

where α_{zz} is the electric polarizability of the ellipsoid in the z direction and $\langle E_z(x)E_z(x)\rangle_{i\xi}$ is the mean-square z component of the electric field fluctuations at position x with imaginary frequency $\omega = i\xi$.

Since the considering geometry is a 3D structure, the calculation is more complex and time consuming. To speed up the computation time, a harmonic expansion technique was applied, which allows Casimir force to be efficiently computed.

2. Maxwell's Stress Tensor and Harmonic Expansion

The method to calculate Casimir forces presented in the time domain involves the modification of Maxwell's stress tensor [6, 7]. Through suitable integration of stress along a close surface with structure enclosed, the force can be obtained as

$$F_i = \int_0^\infty d\omega \oiint_S \sum_j \left\langle M_{ij}(r,\omega)\right\rangle dS_j, \qquad (2)$$

where r is position and ω is frequency. If ω is imaginary frequencies, that is, $\omega = i\xi$, the force can be rewritten as

$$F_i = \mathrm{Im}\int_0^\infty \frac{d\omega}{d\xi} d\xi \oiint_S \sum_j \left\langle M_{ij}(r,\omega)\right\rangle dS_j. \qquad (3)$$

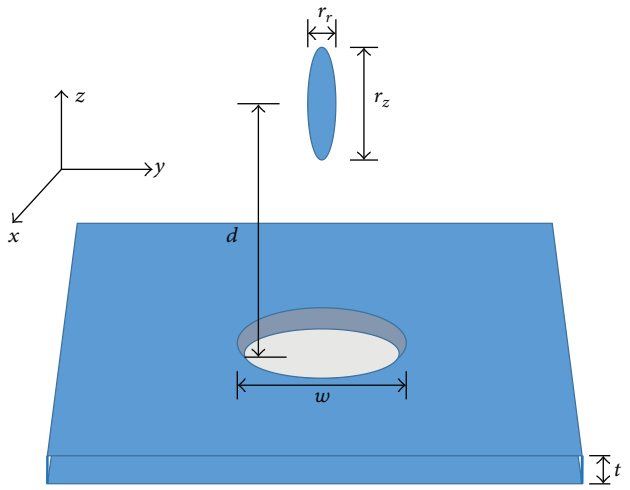

Figure 1: Geometry for achieving Casimir repulsive force: a metal ellipsoid above a thin metal plate with a hole in the center. d is the center-center separation, w is the plate hole width, t is the thickness of the plate, r_r is the minor diameter of the ellipsoid, and r_z is the major diameter of the ellipsoid.

The stress tensor can be explicitly expressed in terms of correlation functions of the field operators $\langle E_i(r,\omega)E_j(r',\omega)\rangle$ and $\langle H_i(r,\omega)H_j(r',\omega)\rangle$ as

$$\begin{aligned}\left\langle M_{ij}(r,\omega)\right\rangle &= \mu(r,\omega)\\ &\cdot\left[\left\langle H_i(r,\omega)H_j\left(r',\omega\right)\right\rangle - \frac{1}{2}\delta_{ij}\sum_k\left\langle H_k^2(r,\omega)\right\rangle\right]\\ &+\varepsilon(r,\omega)\\ &\cdot\left[\left\langle E_i(r,\omega)E_j\left(r',\omega\right)\right\rangle - \frac{1}{2}\delta_{ij}\sum_k\left\langle E_k^2(r,\omega)\right\rangle\right].\end{aligned} \tag{4}$$

The average of the fluctuating electric and magnetic fields in the ground state can easily be obtained as stated in [7, 8].

In a cylindrical symmetry, a practical harmonic expansion basis with $f_n(\mathbf{x})e^{im\phi}$ should be adopted. Thus the resulting fields are separable with ϕ, and the equations only contain the (r,z) coordinates. Now the three-dimensional (3D) problem can be reduced to a two-dimensional problem for each m. Once the fields are determined, the force for each m can be expressed as

$$\begin{aligned}F_{i;m} = \int_0^{2\pi}d\phi\int_S ds_j(\mathbf{x})\,r(\mathbf{x})\,e^{-im\phi}\int_0^{2\pi}d\phi'\int_S ds\left(\mathbf{x}'\right)\\ \cdot r\left(\mathbf{x}'\right)e^{im\phi'}\delta_S\left(\mathbf{x}-\mathbf{x}'\right)\Gamma_{ij;m}\left(t;\mathbf{x},\mathbf{x}'\right),\end{aligned} \tag{5}$$

where $\mathbf{x}$ is three-dimensional coordinates. Now consider that S consists of plane with z = const and r = const, and the detailed expression can be found in [7].

The point source in 3D can be expressed as $f_n(\mathbf{x})e^{im\phi} = \delta(\mathbf{x}-\mathbf{x}')e^{im\phi}$, so the field must have a ϕ dependence of the form $e^{im\phi}$ as follows:

$$\Gamma_{ij;nm}(r,z,\phi,t) = \Gamma_{ij;nm}(r,z,t)\,e^{im\phi}, \tag{6}$$

where $\Gamma_{ij;nm}$ are functions of the electromagnetic fields on the surface S.

Now, we need a geometry-independent function $g(-t)$, resulting from the Fourier transform of $g(\xi)$, which is

$$g(\xi) = -i\xi\left(1+\frac{i\sigma}{\xi}\right)\frac{1+i\sigma/2\xi}{\sqrt{1+i\sigma/\xi}}\Theta(\xi), \tag{7}$$

where $\Theta(\xi)$ is the unit-step function.

Once $g(-t)$ is known, it can be used in time domain to obtain the Casimir force. As discussed in [8]. In the cylindrical system, the time domain $g(-t)$ can be obtained as

$$\operatorname{Im} g(-t) = \frac{1}{2\pi}\left(\frac{2}{t^3}+\frac{3\sigma}{2t^2}+\frac{\sigma^2}{2t}\right). \tag{8}$$

The key point of the approach is to compute the force via a series of independent FDTD calculations in which sources are separately placed at each point on S, calculate the entire frequency spectrum in a single simulation for each source, and then integrate the electromagnetic response in time domain against a predetermined function $g(-t)$ [9, 10]. The final expression of the Casimir force is

$$\begin{aligned}F_i = \int_0^\infty dt\,\operatorname{Im}\left[g(-t)\right]\\ \cdot\sum_n\int_S ds_j(r,z)\,f_n(r,z)\,\Gamma_{ij;n}(r,z,t)\end{aligned} \tag{9}$$

with

$$\begin{aligned}\Gamma_{ij;n}(r,z,t) = \Gamma_{ij;n,m=0}(r,z,t)\\ +2\sum_{m>0}\operatorname{Re}\left[\Gamma_{ij;n,m}(r,z,t)\right].\end{aligned} \tag{10}$$

3. Numerical Results

To demonstrate the validation of our code, we first study a well-known structure of a finite size metallic ellipsoid as sketched in Figure 1. Figure 2 shows the Casimir force with parameters $r_r = 50$ nm, $r_z = 250$ nm, the thickness of plate $t = 100$ nm, the diameter of circular hole on the plate $w = 2\,\mu$m, considering both perfect metal and realistic gold in three different mediums (vacuum, ethanol, and bromobenzene) [11–13]. The force can be computed by our FDTD method in the cylindrical coordinates, with the gold permittivity described by $\varepsilon(\omega = i\xi) = 1+\omega_p^2/\xi^2$, where the plasma frequency ω_p is 1.37×10^{16} rad/s. From Figure 2, we find that the Casimir interaction in golden structure is stronger than metallic objects immersed in vacuum and bromobenzene, and the differences between ethanol are minor, which is in well agreement with the result given in [5].

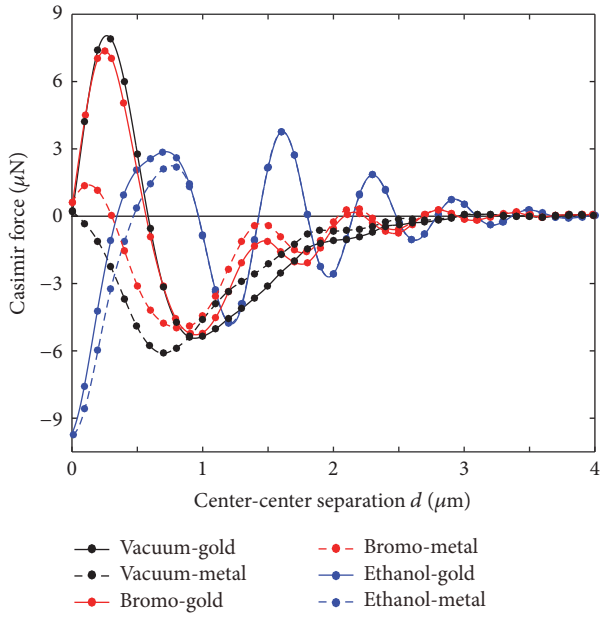

FIGURE 2: Casimir force for ellipsoid-plate geometry with perfect metal and realistic gold in three different mediums, including vacuum, bromobenzene, and ethanol; negative sign represents repulsive force. For $d > 3.5\,\mu$m, forces are close to 0.

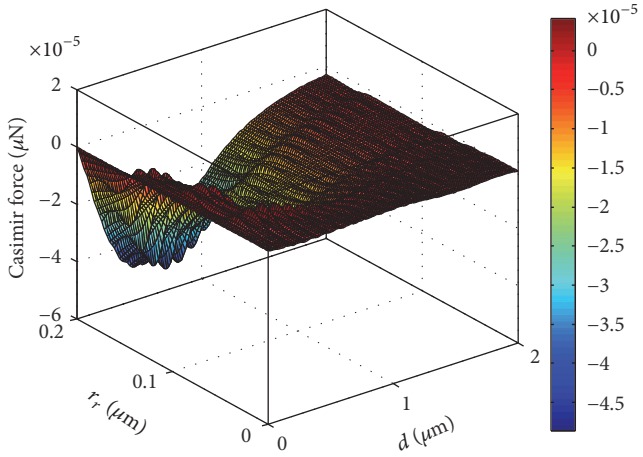

FIGURE 3: The repulsive Casimir force as a function of different minor radius of ellipsoid and different separation between metallic ellipsoid and plate.

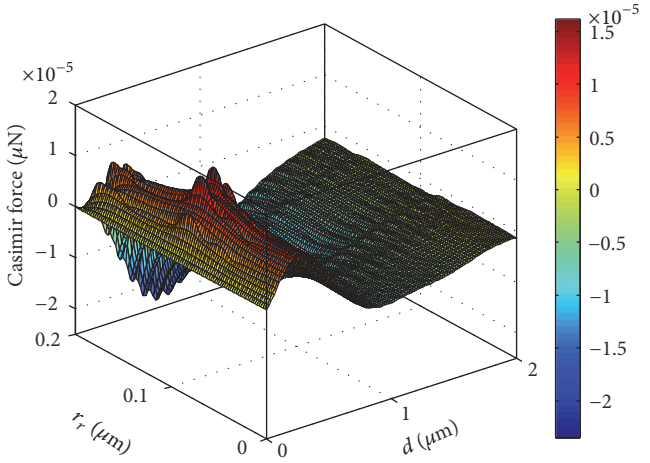

FIGURE 4: The repulsive Casimir force as a function of different minor radius of ellipsoid and different separation between gold ellipsoid and plate.

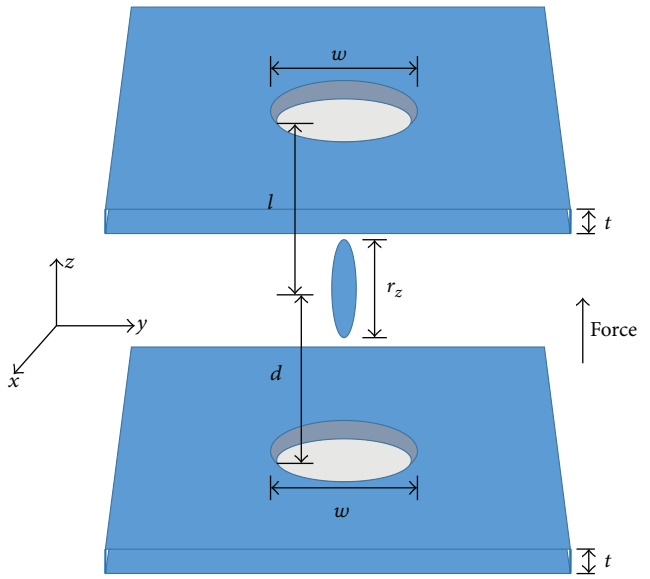

FIGURE 5: New geometry with two plates separately. The parameters are the same as the original geometry (see Figure 1), and the separation between the top plate and ellipsoid is l.

Considering the structure in vacuum again, both ellipsoid and plate are perfect metal and realistic gold; by changing the minor radius of the ellipsoid r_r and the separation between ellipsoid and plate d, the numerical results show that the repulsion between metallic objects (see Figure 3) is stronger than golden ones (see Figure 4).

Until now, the repulsive Casimir force that exists in this special geometry would be appreciated and advocated [14]. It is possible to tune some parameters to obtain applicable force, which can be very useful in practical MEMS. In Figure 5, a new configuration was proposed: one plate with a hole above the ellipsoid and the other plate with a hole below the ellipsoid.

In Figure 6, we discuss how the parameters d and l affect the force in the new configuration. The center of ellipsoid was fixed at $(0, 0, 0)$, the top plate centered at $(0, 0, l)$, and the bottom plate centered at $(0, 0, d)$. Figure 6(a) shows that when the material is gold, we fixed the top plate at some specified l and changed d range from 0 to $4\,\mu$m. If $l < 1.0\,\mu$m, the amplitude of the repulsive force is decreasing with the raise of l. The minimum value of the black line shows that the repulsive force is approximately $10\,\mu$N at $d = 0.9\,\mu$m. The blue line indicates that if $l = 1.0\,\mu$m, the force becomes attractive; the maximum value suggests that

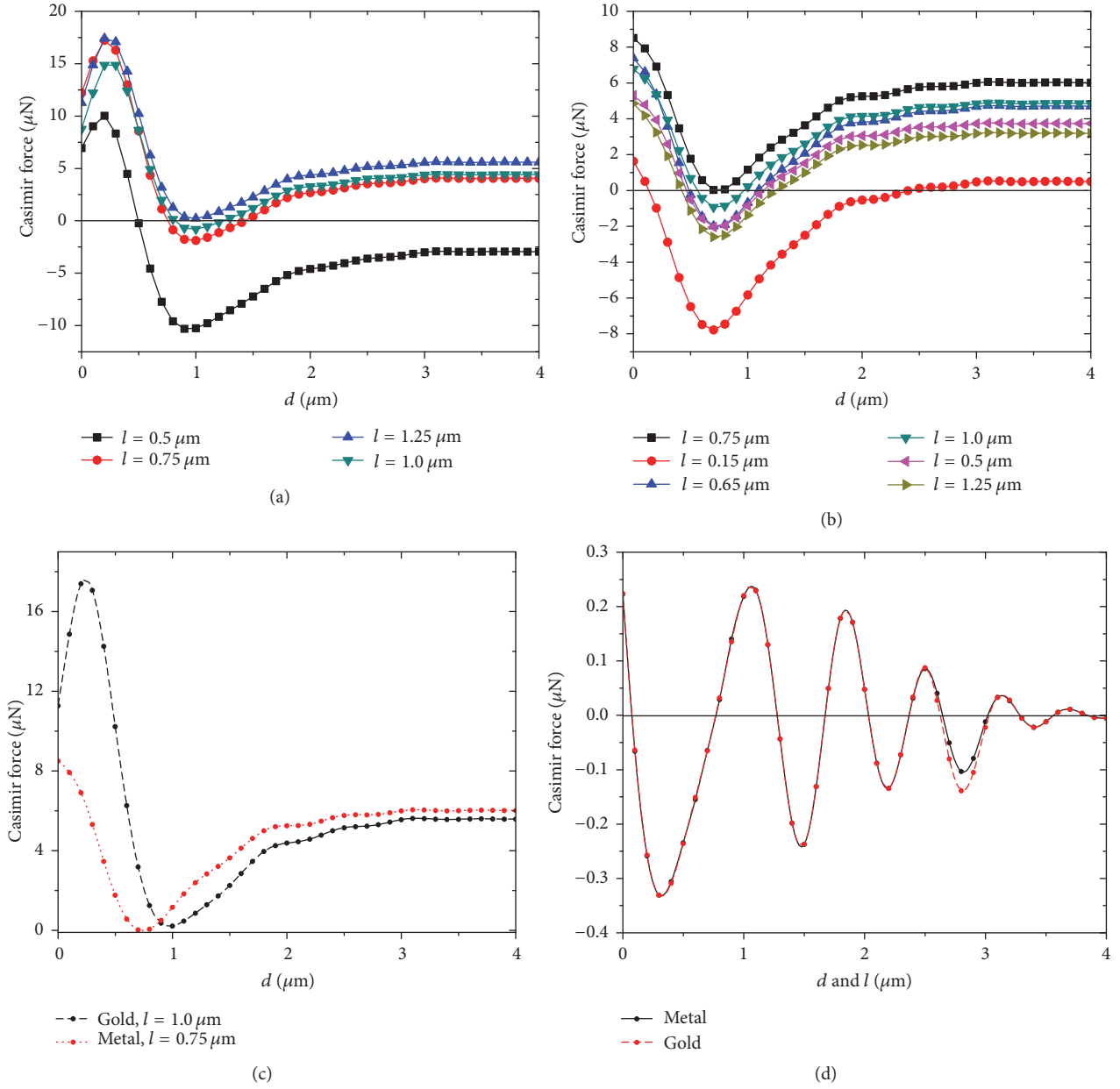

FIGURE 6: The Casimir force in plate-ellipsoid-plate configuration: (a) the material is gold. The black line shows that fixing the ellipsoid and the top plate at $l = 0.5\,\mu$m, the force becomes repulsive with the increase of d. But the blue line indicates that as $l = 1.0\,\mu$m, the force is attractive. The red line and green line suggest that the force is almost attractive; (b) the material is perfect metal, and as $l = 0.75\,\mu$m the force is attractive; (c) shows the two different materials at two different points where the repulsive force becomes attractive; (d) as we fixed the ellipsoid and varied d and l simultaneously, the Casimir force fluctuated between attraction and repulsion.

the attractive force is approximately 18 μN at $d \approx 0.2\,\mu$m. Increasing l continually, as shown in red and green line, the repulsion appears again; the situation of Figure 6(b) is similar to Figure 6(a), but the material is perfect metal. This blue line indicates that if $l = 0.75\,\mu$m, the force becomes attractive. Figure 6(c) shows the two different materials at two different points where the repulsive force becomes attractive. The black dash line suggests that the point of gold material is at $l \approx 1.0\,\mu$m; in contrast, perfect-metal material in red dotted line is at $l \approx 0.75\,\mu$m. Figure 6(d) shows when we fixed the ellipsoid, d and l varied simultaneously. With either gold material or perfect-metal material, the repulsive force and attractive force approach zero.

When we firstly fixed the top plate and the ellipsoid and then started to move the bottom plate, we get the results shown in Figure 6(b). In this case, the total force on the ellipsoid $F = F_b + F_t$, F_t ($-z$ direction) has occurred by the top plate and the ellipsoid; F_b ($+z$ direction) has occurred by the ellipsoid and the bottom plate. Once l was set, F_t was constant value. Then we varied d, the total force F is F_b plus a constant.

The final result can be seen as a linear superposition; thus, the trend of curves is the same as the curve in vacuum in Figure 2. When we increase the separation d and l simultaneously, because $|F_t| = |F_b|$, the two directions are opposite. Thus, the total force on the ellipsoid $F = 0$. But the force fluctuated regularly between positive and negative values because there is a remnant force on the ellipsoid as shown in (d); it is merely the minor interference coming from the two interactive plates. Based on the results of (d), we can make the ellipsoid levitated in vacuum to overcome typical stiction and friction problems in practical MEMS.

4. Conclusion

The FDTD method based on the modification of Maxwell's stress tensor was used to calculate the Casimir force in a cylindrical system, transforming a 3D problem into a 2D problem, which undoubtedly increased the speed and precision of the calculation. A new geometry was proposed to make the ellipsoid levitated between two plates, and then the ellipsoid can be seen as the bearing in practical MEMS.

Competing Interests

The authors declare that they have no competing interests.

Acknowledgments

This project is supported by the National Natural Science Foundation of China (nos. 51277001 and 61471001) and the Key Natural Science Foundation of Anhui Province (no. KJ2010A283).

References

[1] H. B. G. Casimir and D. Polder, "The influence of retardation on the London-van der Waals forces," *Physical Review A*, vol. 73, no. 4, pp. 360–372, 1948.

[2] V. M. Mostepanenko and N. N. Trunov, *The Casimir Effect and its Applications*, Clarendon Press, Oxford, UK, 1997.

[3] E. M. Lifshitz and L. P. Pitaevskii, *Statistical Physics*, part 2, Pergamon Press, Oxford, UK, 1980.

[4] A. W. Rodriguez, F. Capasso, and S. G. Johnson, "The Casimir effect in microstructured geometries," *Nature Photonics*, vol. 5, no. 4, pp. 211–221, 2011.

[5] M. Levin, A. P. McCauley, A. W. Rodriguez, M. T. H. Reid, and S. G. Johnson, "Casimir repulsion between metallic objects in vacuum," *Physical Review Letters*, vol. 105, no. 9, Article ID 090403, 2010.

[6] A. Taflove and S. C. Hagness, *Computational Electrodynamics: The Finite-Difference Time-Domain Method*, Artech House, Norwood, Mass, USA, 2000.

[7] J. Zhang, Z. Huang, and X. Wu, "Casimir force in anisotropic materials with AC Kerr effect," *Progress In Electromagnetics Research M*, vol. 38, pp. 165–173, 2014.

[8] L. S. Brown and G. J. Maclay, "Vacuum stress between conducting plates: an image solution," *Physical Review*, vol. 184, no. 5, pp. 1272–1279, 1969.

[9] A. Rodriguez, M. Ibanescu, D. Iannuzzi, J. D. Joannopoulos, and S. G. Johnson, "Virtual photons in imaginary time: computing exact Casimir forces via standard numerical electromagnetism techniques," *Physical Review A—Atomic, Molecular, and Optical Physics*, vol. 76, no. 3, Article ID 032106, 2007.

[10] A. W. Rodriguez, A. P. McCauley, J. D. Joannopoulos, and S. G. Johnson, "Casimir forces in the time domain: theory," *Physical Review A*, vol. 80, no. 1, Article ID 012115, 11 pages, 2009.

[11] E. M. Lifshitz, "The theory of molecular attractive forces between solids," *Soviet Physics*, vol. 2, no. 1, pp. 73–83, 1956.

[12] G. L. Klimchitskaya, U. Mohideen, and V. M. Mostepanenko, "The Casimir force between real materials: experiment and theory," *Reviews of Modern Physics*, vol. 81, no. 4, pp. 1827–1885, 2009.

[13] P. J. Zwol and G. Palasantzas, "Repulsive Casimir forces between solid materials with high-refractive-index intervening liquids," *Physical Review A*, vol. 81, no. 6, Article ID 062502, 2010.

[14] M. T. H. Reid, J. White, and S. G. Johnson, "Fluctuating surface currents: an algorithm for efficient prediction of Casimir interactions among arbitrary materials in arbitrary geometries," *Physical Review A—Atomic, Molecular, and Optical Physics*, vol. 88, no. 2, Article ID 022514, 2013.